

GT2011-46107

## LIFE ASSESSMENT BY FRACTURE MECHANICS ANALYSIS AND DAMAGE MONITORING TECHNIQUE ON COMBUSTION LINERS

**A. Can Altunlu\*** †

Faculty of Engineering  
Technology, University of  
Twente, P.O. Box 217, 7500 AE  
Enschede, The Netherlands

a.c.altunlu@utwente.nl

**Peter van der Hoogt**

Faculty of Engineering  
Technology, University of  
Twente, P.O. Box 217, 7500 AE  
Enschede, The Netherlands

p.j.m.vanderhoogt@utwente.nl

**André de Boer**

Faculty of Engineering  
Technology, University of  
Twente, P.O. Box 217, 7500 AE  
Enschede, The Netherlands

a.deboer@utwente.nl

### ABSTRACT

A methodology has been developed and tested including a multi-disciplinary framework towards integrated analysis of gas turbine combustors. The sub-elements consist of combustion dynamics, stress and modal analysis, fracture mechanics and structural health monitoring have been interlinked indicating the damage evaluation to life assessment. The interaction between the interrelated combustion driven flame dynamics, acoustic pressure fluctuations and liner wall vibration has been investigated in the laboratory combustor test system. During the operation, the combustion, acoustics and wall vibrations have been coupled together. The dynamic combustion process generates high amplitude pressure oscillations resulting in vibration of the liner structure at about constant elevated temperature in base load operation. The thermo-acoustic instabilities have a significant destructive impact on the life of the liner material due to high cyclic vibration levels at high temperature.

A structural health monitoring (SHM) method has been established to identify the damage, detect the flaw existence and determine the location, severity and progress of the damage for the combustion liners. Vibration-based and acoustic emission (AE) techniques have been applied in the test system to assess the structural behavior. The applicability of the technique has been tested by examining the dynamic modal parameters of the structure. The method enables a reliable assessment on the liner specimen at elevated temperatures by means of non-destructive evaluation under continuous operation of the combustor. The combustion liner specimen material has been assessed by calculating the near-tip fields at the crack tip by finite element based stress and fracture mechanics analysis. An algorithm based on J-Integral has been

utilized to analyze the crack growth behavior under various loading conditions considering both linear and non-linear elastic fracture mechanics concepts. The location and the direction of the cracking on the liner specimen have been predicted. The presented work interrelates the different mechanisms in gas turbine combustors and the applicability of the concepts has been verified and validated in the test systems.

### INTRODUCTION

In modern gas turbines used for power generation, lean premixed combustion technology is generally desired to fulfill the low NO<sub>x</sub> emission targets. However, the gas turbine is susceptible to thermo-acoustic oscillations caused by the combustion driven resultant excessive power loads [1]. Thermo-acoustic instabilities in gas turbine combustors lead to mechanical vibrations by dynamically interacting with the flame dynamics. Consequently, combustion liner material is exposed to the complex damage phenomena. Investigation on the physical damage mechanisms under the complex instability phenomenon is essential to innovate robust designs for combustion systems and provide the safety of power plants. Therefore, an accurate life assessment approach on the hot section components is needed for high efficient lean combustion technologies and reduced emissions while satisfying the structural integrity, durability and reliability of the gas turbine engines.

#### Limit cycles of thermo-acoustic oscillations in gas turbines

The interaction between the turbulent flame, acoustic pressure fluctuations and liner wall vibration has been investigated in the laboratory combustor test system. The combustor test system has a rectangular cross-section in order to locate two windows on the side faces, which enable to

\*Address all correspondence to this author.

†ASME Member.

visualize the dynamic flame behavior and to construct relation between the structural vibrations. Particular combustion operation settings stimulate the acoustic wave propagation to form a coupling between the combustion dynamics and the structural wall vibrations. The variation of the pressure flow field due to flame dynamics creates pressure oscillations that lead to thermo-acoustic instability. In addition, the flame acts as a strong sound source inside the combustor and amplifies the liner vibration amplitudes. The dynamic interdependent interaction within the combustor brings about the limit-cycle pressure oscillations that cause excessive liner wall vibration amplitude leading to the accelerated life consumption. The lifetime of the combustor dominantly linked to the interaction of high amplitude cyclic wall vibrations fatigue damage and elevated temperatures creep damage.

### **Structural health monitoring**

Structural response monitoring and damage or fault detection at the earliest possible stage is crucial to assure the safety of the component, assess the residual lifetime, plan the required maintenance intervals, set inspection requirements. Vibration-based damage identification is a non-destructive method to examine the dynamic properties of the structures. Basically, the vibration-based method tracks the alterations of the modal parameters such as eigenfrequencies, mode shapes, modal damping, modal strain energy and flexibility that indicate the possible damage [2-11]. A non-contact vibration-based damage identification method has been proposed to monitor the health of the combustion liner during operation. The method is based on the modal parameters such as the eigenfrequencies and the mode shapes that are dependent on the physical properties of the structure such as mass and stiffness. The damage can be detected and identified by means of changes in the physical properties affecting the modal parameters due to interrelated fatigue and creep interaction. The method has been utilized and verified for a rectangular flexible plate attached to a stiff rectangular box in the vibration test system. The technique capable to detect the presence of damage, characterize and quantify the severity the damage by examining changes in the measured vibration response of the structure. The location of the damage in the geometry can be determined by pursuing the changes in the measured flexibility of the structure. The localization is based on comparison of the flexibility matrixes using the modes of the intact and the damaged structure. The flexibility matrix [10] is inversely proportional to the square of the natural frequencies; therefore the flexibility matrix is very sensitive to the changes in the low frequency modes of the structure. Furthermore, the remaining service lifetime of the component can be predicted by using a master curve relating number of cycles and life or crack propagation rate.

### **Fracture mechanics**

Gas turbine engine combustors have a variety of feature that can create local stress concentrations. Additionally, cracks and flaws can occur in critical components as material and manufacturing defects or under the operation by oscillating

pressures, elevated temperatures or environmental conditions. Since the presence of cracks/flaws can result in serious degradation of the material strength and structural safety, the engineering structure can fail at a lower stress level than expected. Fracture mechanics is used to calculate stress and deformation fields around a crack tip by considering the influence of the crack existence and crack geometry parameters to the material strength. This approach utilizes the fracture toughness by using stress intensity factors that calculates the critical value of the near-tip fields in linear elastic fracture mechanics. Under extreme operating conditions, the material can undergo significant plastic deformation. Hence an explicit consideration to nonlinear elastic fracture mechanics concepts including plasticity at the crack tip must be done. The magnitude of the stress and deformation fields around the crack tip determines the damage that characterizes the life consumption of the component.

The applicability of a single fracture parameter  $K$  (stress intensity factor) to analyze the crack growth has been shown for several structural materials [12]. The stress intensity factor (SIF) characterizes the stress field around the crack tip as a function of loading condition, specimen and crack geometry. The parameter usage can be utilized in the materials where the plastic work field around the crack tip is limited to small region compared to the crack size despite that the validity of the stress intensity factor is confined to linear elastic stage. The stress intensity factor  $K_I$  has been studied for various cracked geometry configurations and the master curve for various materials has been provided to relate the crack growth rate and stress intensity factor range ( $\Delta K$ ) that are available in the literature [13-15]. Besides, the models based on  $\Delta K$  have been proposed for different crack tip geometries to predict fatigue crack growth [16-18]. The applicability of linear elastic parameter SIF concept is uncertain and unreliable for high temperature crack growth where the plastic flow surrounding the crack tip could not satisfy small yield region condition. J-integral concept [19-22] has been developed as alternative parameter to characterize the crack growth behavior in conditions where the non-linear effects and plastic flow around the crack tip are extensive to alter the crack tip region characteristics and the linear elastic fracture mechanics concepts are invalid. Crack growth behavior under high temperature fatigue using the J-integral concept has been studied considering the superimposed non-linear effects at elevated temperatures such as time dependent creep damage and environmental effects where the linear elastic concepts could be violated at the crack tip region [23]. The J-Integral method can be employed in both linear and non-linear elastic regimes to evaluate the elastic and plastic work fields around the crack tip and the crack growth. Therefore, a fracture mechanics algorithm based on J-Integral concept has been utilized here considering both linear and nonlinear elastic fracture mechanics concepts to analyze the crack growth behavior.

This study is focused on the limit cycle behavior of the unstable oscillations and enhances the mechanistic understanding of the degradation of the gas turbine combustion liners. In addition, a damage detection and monitoring technique has been indicated for the liner structure during the operation. The combustion instabilities cause undesired mechanical vibrations that result in the deterioration on the combustion liner material and the reduction of the liner lifetime. Numerical calculations have been utilized by employing experimentally measured loads to simulate the structural behavior of the liner material under operating conditions. The methodology presented here provides an interdisciplinary tool to correlate the progressive damage in the combustion liner due to the gas turbine engine settings and the reduction in the lifetime due to the elevated vibration amplitudes caused by the thermo-acoustic instabilities.

## METHODOLOGY

### Material

The investigation has been carried out on aluminium plate for validation tests and SS310 steel plate, which is used for liner material in combustor model test system. The aluminum specimen material properties are: Young's modulus ( $E$ ) of 70.5 GPa, Poisson's constant ( $\nu$ ) of 0.3 and a density ( $\rho$ ) of 2700 kg/m<sup>3</sup>. The combustion liner is exposed to elevated temperatures during base-load operation; therefore the influence of the temperature levels on the structural properties becomes crucial. The temperature dependence of Young's modulus and the coefficient of thermal expansion ( $\alpha$ ) are shown for three types of material: a high performance alloy Hastelloy, SS310 and a typical steel grade (Figure 1). The three materials exhibit a dramatically decrease in Young's modulus starting at 400 °C. The steel specimen material properties are; a Poisson's constant ( $\nu$ ) of 0.3 and a density ( $\rho$ ) of 8070 kg/m<sup>3</sup>.

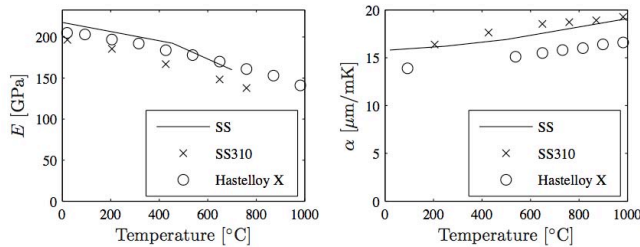


Figure 1. Temperature dependence of Young's modulus ( $E$ ) and the coefficient of thermal expansion ( $\alpha$ ) [24].

The specimen geometry that has been analyzed in this paper (Figure 2) has the width ( $W$ ) 0.16 m, the height ( $2L$ ) 0.21 m. The damaged specimen geometric configurations are presented in Table 1.

Table 1. Damaged specimen configurations.

Damaged plate material	Thickness ( $B$ )	Initial crack length ( $2a$ )	Crack width ( $a_w$ )
Aluminum	0.0011 m	0.035 m	0.003 m
Stainless Steel	0.0010 m	0.010 m	0.003 m

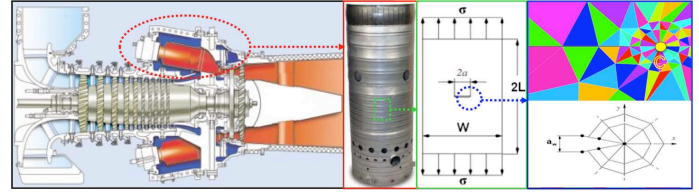


Figure 2. Fracture mechanics on a crack in a gas turbine combustion liner.

### Combustion model test system

A generic model combustor (Figure 6) has been designed as a combustion-driven Rijke tube configuration with steel walls of 1 mm thick [25]. The intention for the investigation on the combustor chamber is to explore and evaluate the damage mechanisms caused by the two-way interaction between the oscillating pressure load in the fluid and the motion of the structure under limit-cycle conditions due to the thermo-acoustic instabilities. The test system provides an understanding on the dynamic interactions between the flame and the structural vibration.

The solid model of the combustor test system and the geometric parameters are depicted in Figure 3 and dimensions are given in Table 2.

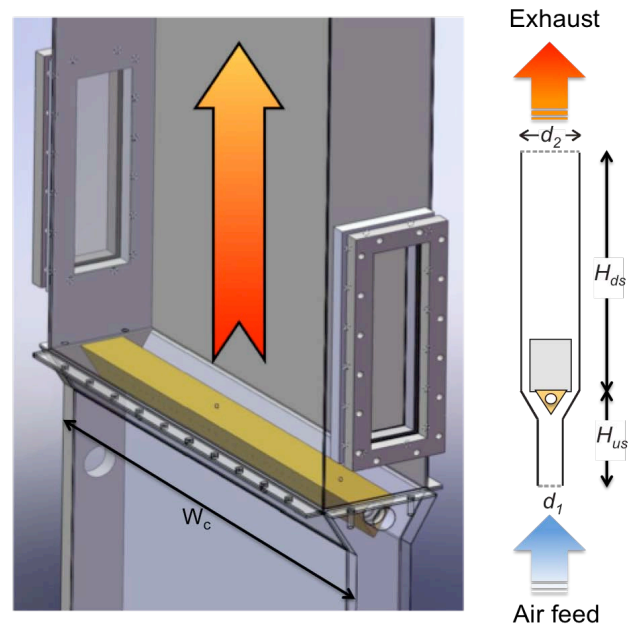


Figure 3. Generic combustor solid model and dimensions.

The combustor test system mainly has two parts, upstream and top sections. The upstream section consists of an air-feeding box, a rectangular duct and a flame holder, which is an equilateral triangular body (bluff body) placed at 1/3rd of the length of the combustor in the downstream section and allows fuel injection through the holes on both sides. The top section consists of a rectangular duct on which there are fixture locations for the quartz glass windows providing an optical access to the downstream of the wedge and the test specimens

for real-time experiments on base-load operation. The windows serve as a visualization tool for the flame and enable to couple the flame with the wall vibrations. Partially premixed type of combustion occurs in the combustor test system. Methane (CH<sub>4</sub>) is used as the fuel at room temperature with no preheating. The ignition occurs just above the surface of the wedge where the flame stabilization takes place on the wedges wake. The test system is supported on three locations. The first support is located at the burner exit plane and the other two are 370 mm and 1000 mm above the plane.

Table 2. Combustor test system dimensions.

H <sub>us</sub>	Upstream height [mm]	322
H <sub>ds</sub>	Downstream height [mm]	1106
W <sub>c</sub>	Combustor width [mm]	220
d <sub>1</sub>	Depth of upstream [mm]	52
d <sub>2</sub>	Depth of downstream [mm]	27
B <sub>c</sub>	Wall thickness [mm]	1.0

### Vibration monitoring test system

The structural response of the intact and damaged specimens has been explored in the vibration monitoring test system shown in Figure 4. The test system consists of a hollow aluminum box with 30 mm thick walls, a 30 mm thick plate to cover the top of the box and an excitation source, loudspeaker. The design serves as a highly stiff structure to avoid any interaction between the specimen and test box whose first eigenfrequency is 1270 Hz (Figure 5). The flexible aluminum plate specimen with 1.1 mm thickness has been attached to the box by reinforcement strips bolted to the box that satisfies clamped on all edges condition. The loudspeaker inside the box generates an interior sound field resulting in vibration on the flexible plate [26]. The surface velocity of the specimen has been scanned by a laser sensor and programmable transverse system.

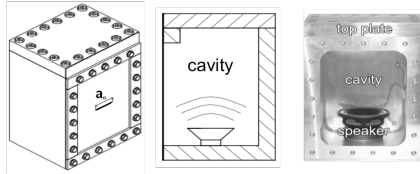


Figure 4. The test setup covered by a flexible plate and the excitation configuration.

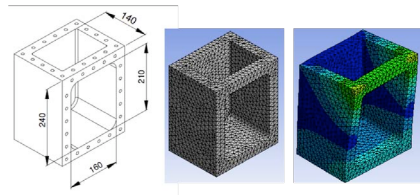


Figure 5. Dimensions of the box (left), and the first mode shape of the bare frame (1270 Hz).

The experiments have been performed in the stiff box with well-defined test and boundary conditions. Therefore, the tests under the intact and damaged conditions provide a basic

understanding on the relation between eigenfrequencies, mode shapes, flexibility and crack growth. The technique is suitable to monitor the damage at high temperatures on the specimen material, which is placed at the specimen holders in the generic combustor test system (Figure 6). The technique enables to detect the damage locally and globally and defines the location and severity of the damage or multiple damages. The vibration-based damage evolution monitoring on the system consists of a laser doppler vibrometer (1), a traverse system (2), a combustor (3) and windows or specimen holder (4).

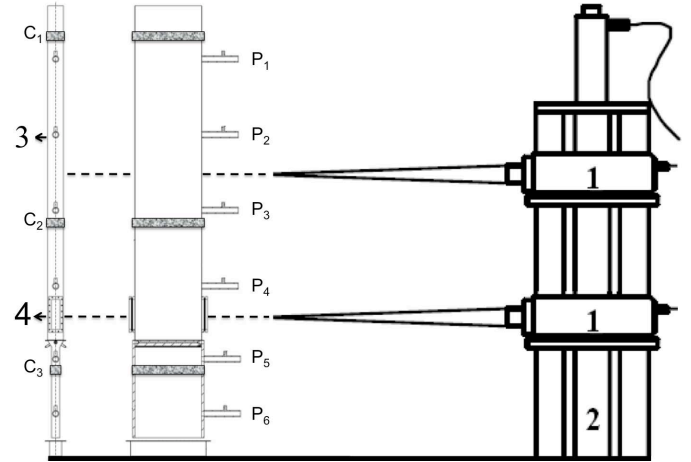


Figure 6. Vibration-based damage evolution monitoring (C: clamping positions, P: pressure transducer positions).

### Theory, procedure and solution in fracture mechanics

A finite element analysis was performed to characterize and calculate stress and strain distributions around the crack tip. The near-tip fields provide a measure of the material degradation on the progressive damage under gas turbine engine operation. The approach of the fracture mechanics concept for combustors is depicted in Figure 2 and the algorithm employed in the sub-domain of interest is presented in Figure 9.

The limit of the linear regime for a material behavior prior to the crack propagation is defined by the stress intensity factor, which describes the intensity of the stress distribution around the crack tip. The numerical accuracy for the stress intensity factor calculation has been validated by the equation developed by Feddersen [27].

$$K = S\sqrt{\pi a}F \quad (1)$$

$$F = [\sec(\pi a/W)]^{1/2} \quad (2)$$

where  $F$  is the boundary-correction factor,  $S$  is the applied stress,  $W$  is the specimen width and  $a$  is the half-crack length. The solution for  $K$  has been extended by the equation developed by Tada [28].

$$F = [\sec(\pi a/2)]^{1/2} [1 - 0.025\alpha^2 + 0.06\alpha^4] \quad (3)$$

where  $\alpha_K = 2a/W$ .

The J-Integral, which is a path-independent line integral, describing the strain energy release rate [19], has been used as the criterion for the crack propagation stage on the geometry containing a central crack. Hutchinson [20] and Rice and Rosengren [21] showed that the J-Integral characterizes the stress and deformation fields at the crack tip region of a stable crack for elastic-plastic material. The J-Integral calculation is based on the domain integral method, which applies area integration for 2-D analysis described by Shih [22] and provides a measure of the intensity of crack-tip strain field in the cracked body. The strain energy density of the material,  $W(\epsilon)$ , with stresses given by

$$W = W(x, y) = W(\epsilon) = \int_0^\epsilon \sigma_{ij} d\epsilon_{ij} \quad (4)$$

$$\sigma_{ij} = \frac{\partial W}{\partial \epsilon_{ij}} \quad (5)$$

A small strain deformation theory of plasticity material model is assumed and the stress is described as a function of only the strain state shown in Eq. (5), where  $\epsilon = [\epsilon_{ij}]$  is the infinitesimal strain tensor. When a body contains a crack shown in Figure 7 having a crack face parallel to the x-axis is considered, the expression for two-dimensional path independent integral J is

$$J = \int_{\Gamma} (W dy - \mathbf{T} \cdot \frac{\partial \mathbf{u}}{\partial x} ds) \quad (6)$$

where  $\Gamma$  is a curve enclosing the crack tip in a counterclockwise direction,  $\mathbf{T}$  is the traction vector on  $\Gamma$  defined according to the outward normal,  $\mathbf{T}_i = \sigma_{ij} n_j$ ,  $n_j$  is the vector of the outward unit normal  $\mathbf{n}$  to the curve  $\Gamma$ ,  $\mathbf{u}$  is the displacement vector, and  $ds$  is an element of  $\Gamma$ .

In a generalized nonlinear elastic material, the J-integral can be physically interpreted as the rate of change of potential energy,  $U$ , caused by crack extension and expressed as

$$J = -\frac{1}{B} \frac{\partial U}{\partial a} \quad (7)$$

where the energy change is measured at any given displacement. In the linear elastic regime, the J-Integral reduces to the strain energy release rate,  $G$  (for small-scale yielding condition) that is also referred as the crack driving force. Therefore the stress intensity factor can be evaluate as

$$J_I = G_I = \frac{K_I^2}{E^*} \quad (8)$$

where  $E^* = E$  for plane stress.

$$K_I = \sqrt{J_I E} \quad (9)$$

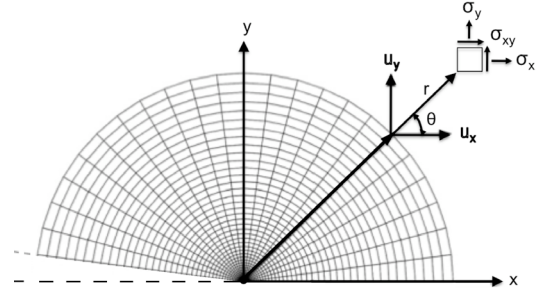


Figure 7. The stresses ahead of the crack tip with mesh contours.

$$\sigma_{ij} = \frac{K}{\sqrt{2\pi r}} f(\theta_{ij}) \quad (10)$$

where  $K$  is the stress intensity factor,  $r$  and  $\theta$  are the polar coordinates.

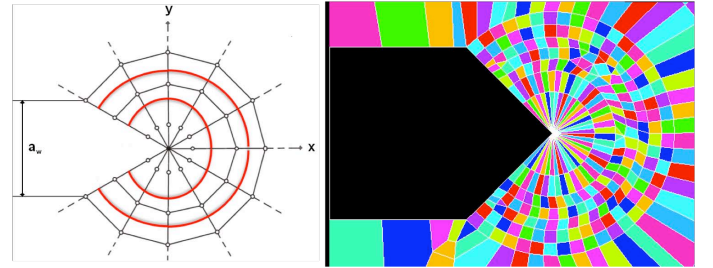


Figure 8. Crack tip refined spider mesh.

A Half symmetric model has been analyzed by illustrating the both crack faces. The spider mesh (Figure 8) scheme has been used around the crack tip region and the crack tip has been selected as a concentration point of the refined mesh at the tip region to handle rapidly varying stress and deformation fields [29]. The crack propagation procedure is based on the duplication and separation method on the nodes along the pre-defined crack path history.

Nonlinear elastic plastic stress analysis and fracture mechanics parameter calculation run collaboratively in the fracture analysis. The numerical algorithm is presented in Figure 9. The stress intensity factor ( $K_I$ ) at the crack tip has been calculated and compared to the material fracture toughness ( $K_{IC}$ ) to determine the linear regime limit of the material. When the nonlinear state is satisfied, the J-Integral method has been used to predict  $J_I$  from path integration in the crack tip region. The crack opening displacement procedure has been employed to apply the relative displacement of the coincident crack faces with respect to J-Integral calculation [30]. The crack propagates towards the perpendicular direction of the first principal stress direction at the crack tip. The crack tip re-meshed with spider mesh procedure at each crack extension step to create calculation contours around the crack tip. The iterative procedure continues until the critical limit that results in failure.

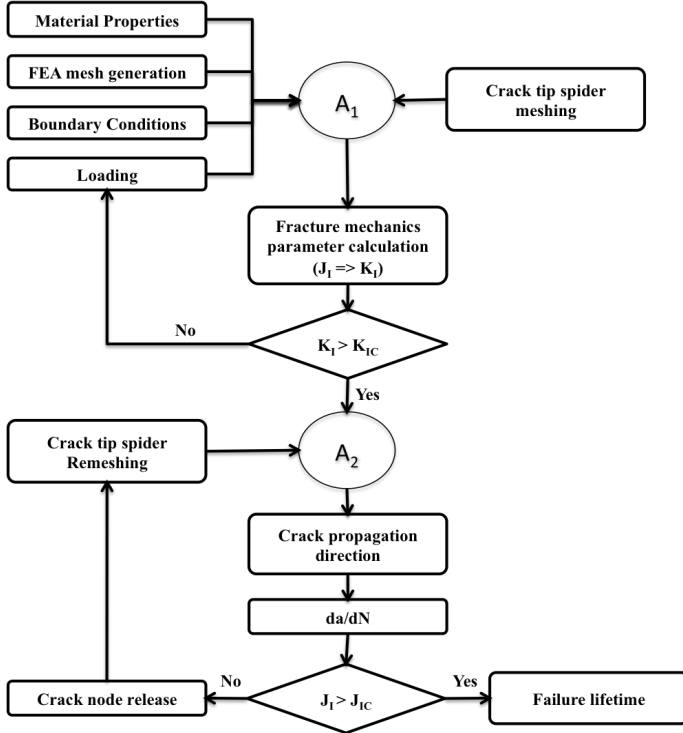


Figure 9. Fracture mechanics algorithm.

## RESULTS

### Vibration monitoring test system

The experiments have been performed on the aluminum flexible intact and damaged plate to examine the dynamic modal parameters (eigenfrequencies, mode shapes and flexibility). The robustness of the test system and methodology has been accurately satisfied. The analytical, numerical and experimental results for eigenfrequencies are listed in Table 4 and mode shapes are depicted in Figure 10 for the intact plate. The alteration on eigenfrequencies of the intact and damage plate are presented in Table 5. The first seven eigenfrequencies decrease as the damage is employed in the specimen and vibration-based and acoustic-based monitoring techniques are in good agreement. The eigenfrequencies of the first five modes of the rectangular plate has been analytically calculated by [31]

$$f_{ij} = \frac{\lambda_{ij}^2}{2\pi a_p^2} \sqrt{\frac{Eh_p^3}{12\gamma(1-\nu^2)}} \quad (11)$$

where  $\lambda_{ij}$  is the dimensionless frequency parameter of rectangular plates which is a function of the boundary conditions applied to the plate, the aspect ratio of the plate tabulated by length to width ratio,  $a_p$  is the length and  $h_p$  is the thickness of the plate,  $\gamma$  is the mass per unit area of the plate ( $\gamma = \mu * h$  with density  $\mu$ ). The aspect ratio of the flexible plate is 0.762 and the  $\lambda_{ij}^2$  values were interpolated between aspect ratios of 2/3 and 1.0. The  $\lambda_{ij}^2$  values for clamped on all edges are listed in Table 3.

Table 3. The interpolated values for  $\lambda_{ij}^2$ .

	Mode Sequence				
	1	2	3	4	5
$\lambda_{ij}^2$	29.58	50.8	68.22	78.49	94.64
(ij)	S(1,1)	S(1,2)	S(2,1)	S(2,2)	S(1,3)

The deviation on the eigenfrequencies of the plates for the analytical calculation was caused by the interpolation of the  $\lambda_{ij}$  values from the literature and for the numerical calculations the solid modeling of the crack geometry has smoother features than the artificial crack machined into the specimen.

Table 4. Eigenfrequencies [Hz] of the intact plate.

Mode No	Analytic	FEA	Measure (Vibration-based)	Deviation [%] of FEA
1	310	302	304	-0.66
2	532	513	515	-0.39
3	714	706	701	-0.71
4	822	858	858	0.00
5	991	900	901	-0.11

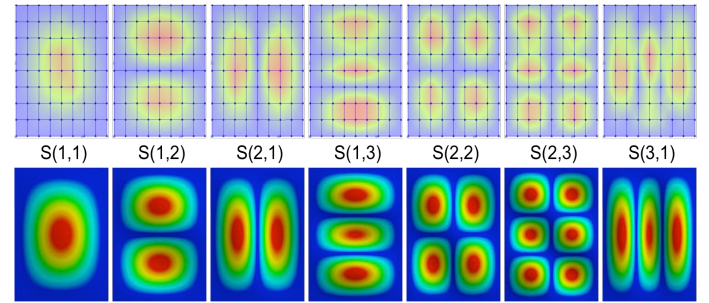


Figure 10. Experimental (above) and numerical (below) results for mode shapes of the flexible plate.

Table 5. Eigenfrequencies [Hz] of the intact and damaged plate.

Mode No.	Intact Plate (Vibration-based)	Damaged Plate (Vibration-based)	Damaged Plate (Acoustic-based)	Damaged Plate (FEA)
1.	304	299	300	286
2.	515	509	510	474
3.	701	693	694	699
4.	858	838	837	753
5.	901	900	898	889
6.	1235	1227	1225	1015
7.	1310	1282	1283	1194

A sensitivity analysis on the eigenfrequencies due to the damage (center crack) is shown in Figure 11, which indicates the most sensitive mode number to the damage. Mode 4 has been found to give the most distinguishable response for capturing the small changes in the dynamic structural properties.

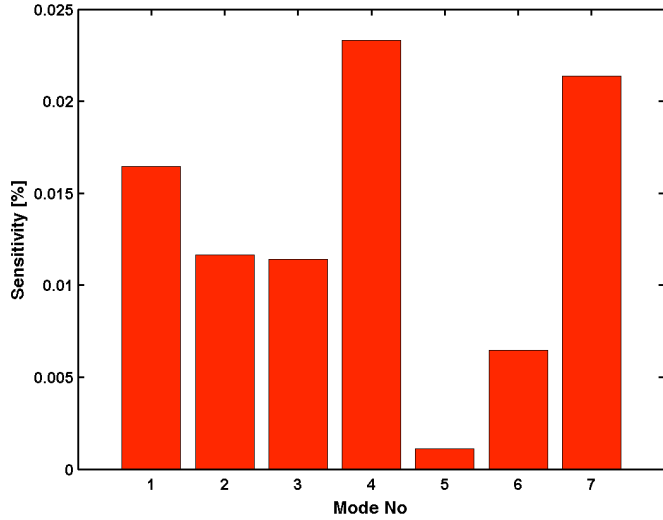


Figure 11. Sensitivity analysis on eigenfrequencies.

### Damage identification and localization

The damage on the flexible aluminum plate has been detected and localized by the flexibility method [9-11] using by the vibration-based laser measurements. The surface response of the specimen alters as damage occurs in the specimen by affecting the local flexibility of the structure. The damage location has been extracted from 9x9 laser sensor measurement grid scans on the rectangular plate is shown in Figure 12. The flexibility matrix [10] related to the modal data is given

$$F = \Phi \Omega^{-1} \Phi^T = \sum_{i=1}^n \frac{1}{\omega_i^2} \Phi_i \Phi_i^T \quad (12)$$

where  $F$  is the flexibility,  $i$  is the mode shape number indicator,  $n$  is the number of degrees of freedom,  $\Phi = [\Phi_1, \Phi_2, \dots, \Phi_n]$  is the mode shape matrix,  $\omega$  is the modal frequency and  $\Omega = \text{diag}(\omega_i^2)$  is the modal stiffness matrix.

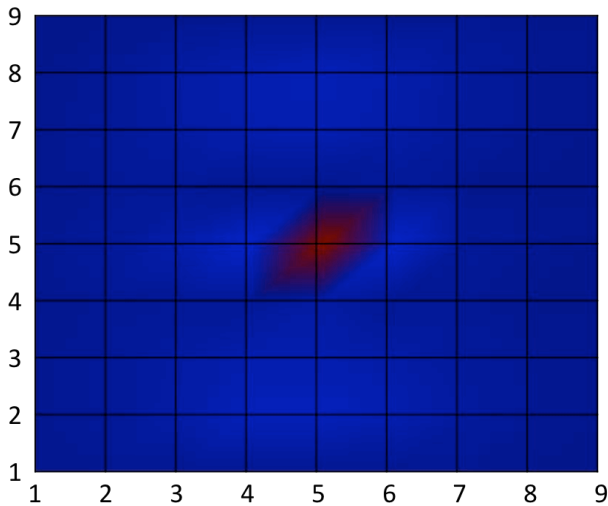


Figure 12. Damaged detected by vibration based measurements.

### Investigation on combustion liner material

Numerical investigation has been carried out on the SS310 material, which is a specimen material on the generic combustor test system. The results for the intact and damaged plate as well as for the hot operating conditions at 400°C are presented in Table 6. Mode number 4 has been identified as the most sensible mode to the damage by the sensitivity analysis (Figure 13).

Table 6. Eigenfrequencies [Hz] of the intact and damaged steel plate at room temperature and at 400°C.

Mode No.	Intact Plate (FEA)	Intact Plate (at 400°C) (FEA)	Damaged Plate (FEA)	Damaged Plate (at 400°C) (FEA)
1.	270	254	269	252
2.	458	431	458	430
3.	632	594	631	594
4.	767	721	754	709
5.	805	757	805	756
6.	1098	1031	1097	1031
7.	1182	1111	1179	1109

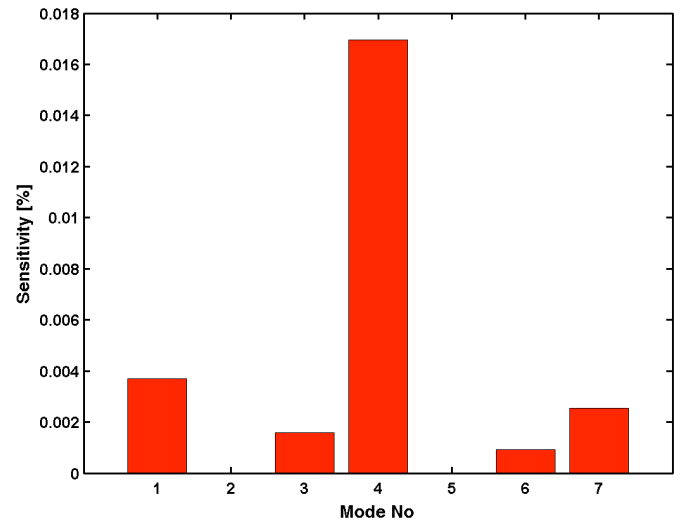


Figure 13. Sensitivity analysis on eigenfrequencies.

### Fracture mechanics on the near-tip field

The damage evaluation analysis has performed considering both linear and non-linear elastic fracture mechanics concepts in the combustion liner stainless steel material by calculating the fracture parameters and the near-tip field around the crack tip region. The path independent fracture parameter J-Integral calculation has been utilized in both the linear and nonlinear regime. The convergence of the calculated  $J_I$  values with respect to the number of contours in the spider mesh around the crack tip is presented in Figure 14. The  $J_I$  value tends to converge after four contours calculation that provides satisfactorily validity on the stress intensity factor under 50 MPa applied load. Therefore  $J_I$  has been calculated using four contours around the crack tip in the further investigation.

The stress intensity factor provides a description of the crack tip stress field unless immoderate loading violates the small scale yielding assumption. The SIF values have been calculated using the J-Integral method under several applied loads and the results have been compared with Feddersen [27] and Tada [28] equations (Figure 15). Comparing the numerical and the analytical results on SIF values have given the transition level from linear to non-linear regime. The threshold has been chosen as 200 MPa applied load for further analysis to satisfy the non-linear computation requirement.

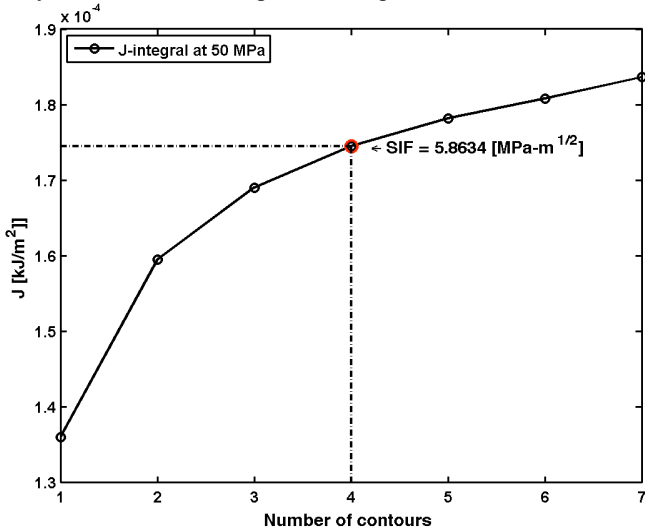


Figure 14. J-Integral calculation convergence.

The von Mises plastic strain values have been calculated at the crack tip and the neighbor node locations in the crack tip region under 200 MPa loading in order to examine the non-linear regime in the simulation. As seen from Figure 16, the von Mises plastic strain amplitudes decrease as the distance increases between the target node and crack tip node.

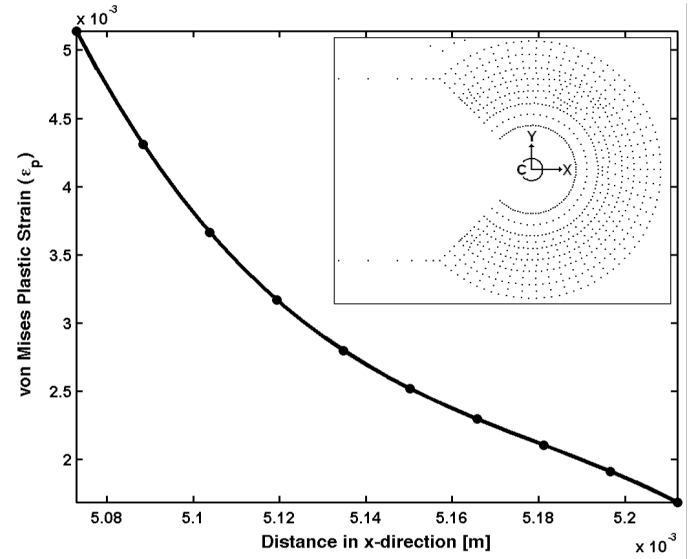


Figure 16. The crack near-tip field amplitudes.

In the nonlinear elastic regime, the plastic flows surrounding the crack tip cannot hold the small yield region condition. Therefore the plasticity around the crack tip results in local softening of the material and induces the crack driving mechanism. The plastic work done of a growing crack dissipates as thermal energy and reshapes the internal state of the material. The dissipation of the plastic work generates thermal fields around the crack tip that promotes localization of deformation.

The von Mises plastic strain field (Figure 17) localized and intensified around the crack tip; on the other hand the elastic strain field (Figure 18) spread through a larger field with smaller amplitudes compare to the plastic strain field.

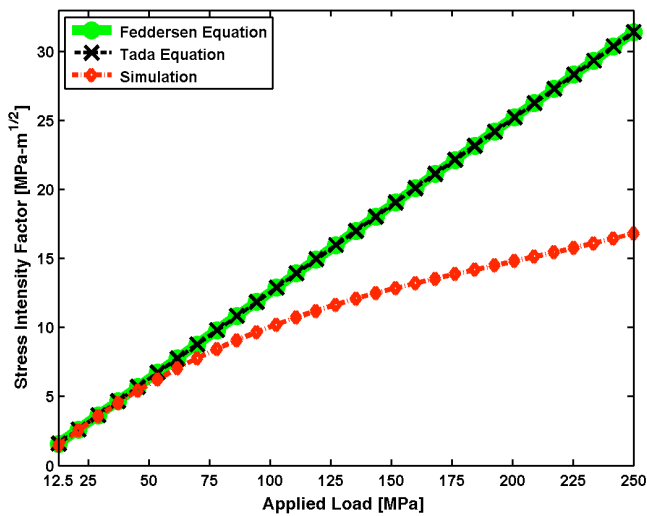


Figure 15. Validity of stress intensity factor

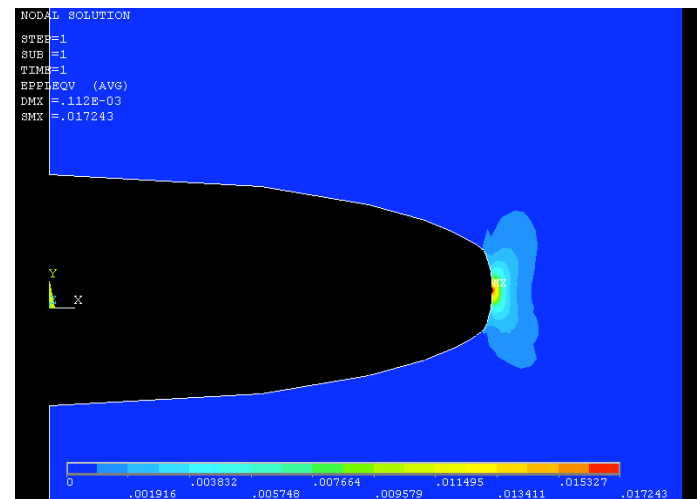


Figure 17. von Mises plastic strain field at the crack tip.

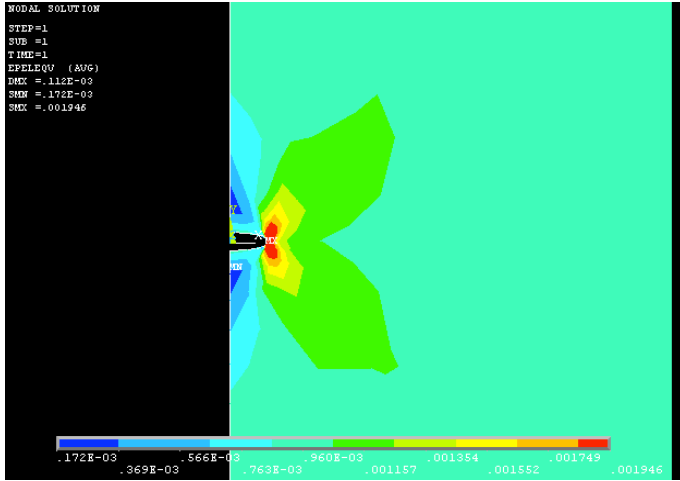


Figure 18. von Mises elastic strain field at the crack tip.

The  $J_I$  versus crack extension [ $J_I=J_I(\delta a)$ ] relation has been numerically evaluated and indicated in Figure 19. The  $J_I$  amplitude at the crack tip tends to increase with respect to Mode I stable crack propagation.

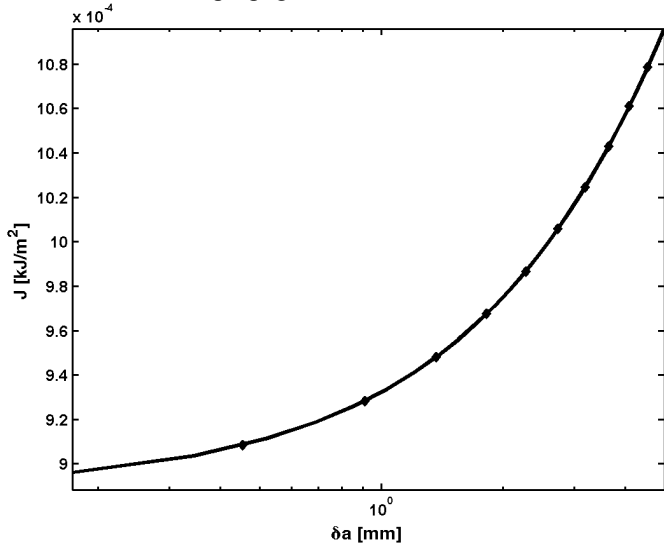


Figure 19.  $J_I$  values for crack extension ( $\delta a$ ).

**Combustor model test system**

An experiment has been performed on the combustor test system at 50 kW and an air excess ratio coefficient of 1.40 by operating conditions. The wall vibration velocity has been measured by a laser doppler vibrometer. The vibration frequency matches the acoustic frequency that has been recorded using pressure transducers shown in Figure 6. Pressure and wall vibration velocity measurements in time and frequency domain are depicted in Figure 20. A typical limit cycle characteristic can be seen in time domain and the peak frequency about 100 Hz on auto-spectrum plot that overall profile shows limit cycle oscillations [32].

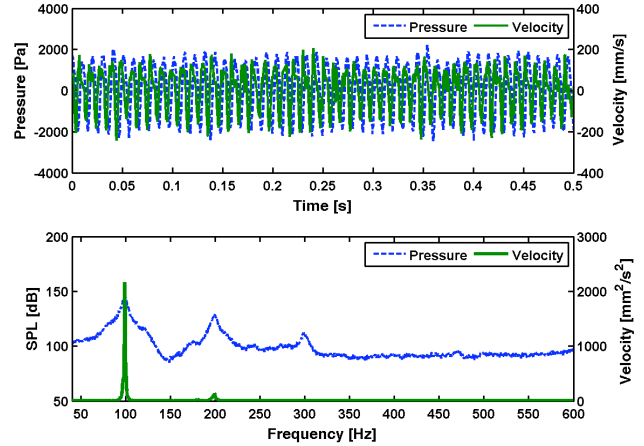


Figure 20. Time signal and auto-spectrum for acoustic pressure and velocity of the wall on combustor test system.

The combustor liner material is exposed to elevated temperatures during the operation; hence the temperature dependence of the material properties must be considered. The eigenfrequencies of a plate scale by the root of Young’s modulus (Eq. 11). Young’s modulus of the liner material decreases approximately 15% as the temperature increases from room temperature to 400°C. Thus the eigenfrequencies decrease approximately 8%. As the eigenfrequencies of the combustion liner are scaled down by 8% (Table 7), a coupling between the structural eigenfrequency and the operational acoustic frequency occurs that leads to limit cycle state in the combustor.

Damaged case of the combustor liner structural behavior has been investigated numerically at room temperature. A through thickness central crack has been located at one of the front walls of the liner (Figure 6) on the mid-level of the side windows. Damaged situation is compared with the damaged situation by analyzing eigenfrequencies (Table 7) and modes shapes (Figure 21). The mode shapes were reshaped and rearranged in damaged situation and modal frequencies inclined to alter particularly in damage part compare to the intact liner. The liner damage has created a reformed situation in the dynamic modal properties and has intended to point out the most sensitive parameter to accurately monitor the structure during the operation and detect and identify the possible damage.

Table 7. Eigenfrequencies [Hz] of intact and damaged combustion liner.

Mode	Intact Liner [Hz]	Damaged Liner [Hz]	Deviation [%]
1.	92	92	0
2.	106	106	0
3.	108	115	-6.5
4.	114	124	-8.8
5.	121	127	-4.9
6.	127	146	-14.9
7.	146	149	-2.1

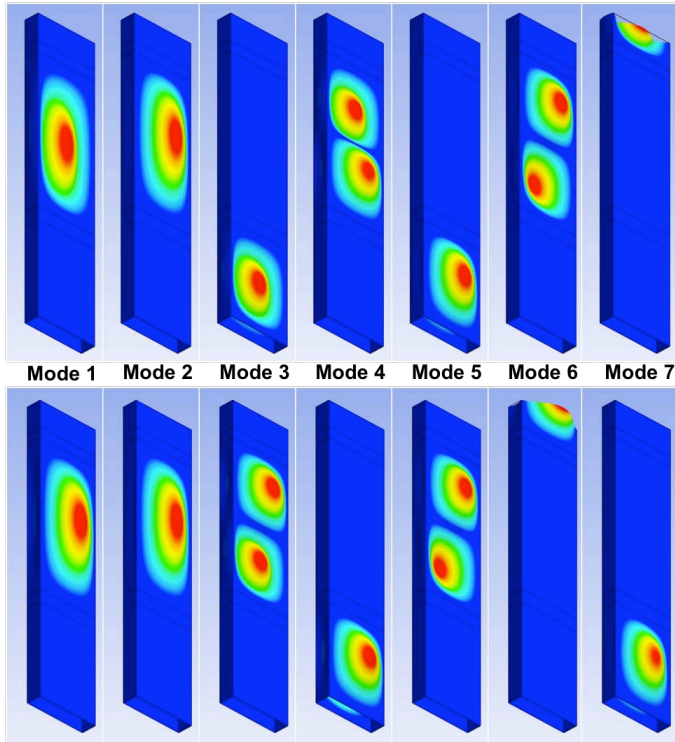


Figure 21. Mode shapes of combustion liner: intact (top) and damaged (bottom).

## CONCLUSIONS AND DISCUSSIONS

In this work, a methodology is presented concerning the multi-disciplinary framework towards integrated analysis of gas turbine combustion liner life assessment. The elements of multi-disciplinary framework consist of combustion dynamics, stress and modal analysis, fracture mechanics, structural health monitoring and their convergence to life assessment. The applicability of the proposed complementary approach to combustion liners has been highlighted by numerical and experimental verification and validation on the vibration monitoring test system. The vibration test system has been chosen because of its simplicity, well-defined boundary condition and robustness towards integrating the method to the combustor test system.

The results of the structure monitoring experiments show that the technique can be used in damage detection, localization and quantification on the specimens. The non-contact monitoring method enables to monitor the health of the specimen located in the generic combustor test system during the regular operation. The technique overcomes the challenges of elevated temperature conditions, high amplitude loading and harsh environment conditions of combustion process. The method is able to identify the crack initiation and propagation by monitoring the changes of the most sensible eigenfrequency of the structure to damage.

The residual lifetime of a cracked structure under plane stress conditions has been evaluated for ductile specimen considering both the effects of plasticity and stable crack

propagation. On stable crack growth prior to failure, the metallic material exhibits localized plasticity at the crack tip creating a plastic zone and the strain magnitude decreases as a function of the crack tip distance.

The calculated plastic work fields formed by the crack tip extension generate thermal energy due to plasticity. The corresponding temperature fields around the crack tip results in softening of the material [33]. The dissipation of the heat ahead of the crack tip quantified by the crack propagation gradually indicates the damage evolution in the material. This information, which is linked to the life consumption of the material, is vital for providing structural integrity, durability and reliability in critical components in gas turbines.

It should be noted that the variation of thermal expansion coefficient due to the temperature change causes pre-stress effect. The generic combustion test system specimen holder on the liner enables the specimen to slide inside the fixture due to expansion in longitudinal and transverse directions. This mechanism partially reduces the thermal expansion, however pre-stress can still remain due to the friction. Consequently, the variation of elastic modulus has been taken into account on the numerical calculations of eigenfrequencies at 400°C.

## NOMENCLATURE

$E$	Young's modulus
$\nu$	Poisson's ratio
$\alpha$	Coefficient of thermal expansion
$W$	Width
$2L$	Height
$B$	Specimen thickness
$2a$	Crack length
$a_w$	Crack width
$K_I$	Stress intensity factor (SIF)
$K_C$	Fracture toughness
$\Delta K$	Stress intensity factor range
$J_I$	J-integral value
$F$	Boundary-correction factor
$G$	Strain energy release rate
$S$	Applied stress
$\alpha_K$	Geometrical ratio
$\lambda_{ij}$	Dimensionless frequency parameter

## ACKNOWLEDGMENTS

The authors would like to acknowledge the funding of this research by the EC in the Marie Curie Actions – Networks for Initial Training, under call FP7-PEOPLE-2007-1-1-ITN, Project LIMOUSINE with project number 214905.

## REFERENCES

- [1] R. A. Huls, A. X. Sengissen, P. J. M. van der Hoogt, J. B. W. Kok, T. Poinsot, and A. de Boer, "Vibration prediction in combustion chambers by coupling finite elements and large eddy simulations", *Journal of Sound and Vibration* 304, 224 – 229, (2007).

- [2] P. Cawley and R.D. Adams, "The locations of defects in structures from measurements of natural frequencies" *Journal of Strain Analysis*, 14, 49–57, (1979).
- [3] N. Stubbs and R. Osegueda, "Global non-destructive damage evaluation in solids", *Modal Analysis: The International Journal of Analytical and Experimental Modal Analysis*, 5, 67–79, (1990).
- [4] O. S. Salawu, "Detection of structural damage through changes in frequency: a review" *Engineering Structures*, 19, 718-723, (1997).
- [5] W.M. West, "Illustration of the use of modal assurance criterion to detect structural changes in an orbiter test specimen", in: *Proceedings Air Force Conference on Aircraft Structural Integrity*, 1–6, (1984).
- [6] R.L. Mayes, "Error localization using mode shapes—an application to a two link robot arm" in: *Proceedings 10th International Modal Analysis Conference*, 886–891, (1992).
- [7] N. Stubbs, J.T. Kim, and C.R. Farrar, "Field verification of a nondestructive damage localization and severity estimation algorithm", in: *Proceedings of the 13th international modal analysis conference*, 210–218, (1995).
- [8] T. H. Ooijevaar, R. Loendersloot, L.L. Warnet, A. de Boer, R. Akkerman, "Vibration based structural health monitoring of a composite t-beam", *Composite Structures*, 92, 2007–2015, (2010).
- [9] T. Toksoy and A. E. Aktan, "Bridge-condition assessment by modal flexibility", *Experimental Mechanics*, 34, 271–278, (1994).
- [10] A. K. Pandey and M. Biswas, "Damage detection in structures using changes in flexibility," *Journal of Sound and Vibration*, 169, 3–17, (1994).
- [11] A. K. Pandey and M. Biswas, "Damage diagnosis of truss structures by estimation of flexibility change", *Modal Analysis: The International Journal of Analytical and Experimental Modal Analysis*, 10, 104-117, (1995).
- [12] G.R. Irwin, *Trans ASME* 79, 361 (1957).
- [13] J.E. Srawley and W.F. Brown, "Fracture toughness testing", *Symposium on fracture toughness testing and its applications*, Pa: American Society for Testing and Materials, ASTM STP 381, 133-198, (1965).
- [14] P.C. Paris and G.C. Sih, "Stress analysis of cracks", *Symposium on fracture toughness testing and its applications*, Pa: American Society for Testing and Materials, ASTM STP 381, 30-83, (1965).
- [15] W.F. Brown and J.E. Srawley, "Plane strain crack toughness testing of high strength metallic materials", Pa: American Society for Testing and Materials, ASTM STP 410, (1966).
- [16] N.E. Frost and J.R. Dixon, "A theory of fatigue crack growth", *International Journal of Fracture Mechanics*, 3, 301-316, (1967).
- [17] N.E. Frost and J.R. Dixon, "A fracture mechanics analysis of fatigue crack growth data for various materials", *Engineering Fracture Mechanics*, 3, 109-126, (1971).
- [18] L.P. Pook and N.E. Frost, "A fatigue crack growth theory", *International Journal of Fracture*, 9, 53-61, (1973).
- [19] J.R. Rice, "A path independent integral and the approximate analysis of strain concentration by notched and cracks", *Journal of Applied Mathematics* 35, 379-386, (1968).
- [20] J.W. Hutchinson, "Singular Behavior at the End of a Tensile Crack in a Hardening Material", *Journal of the Mechanics and Physics of Solids* 16, 13-31, (1968).
- [21] J.R. Rice and G.F. Rosengren. "Plane strain deformation near a crack tip in a power law hardening material", *Journal of the Mechanics and Physics of Solids* 16, 1-12, (1968).
- [22] C.F. Shih, B. Moran, and T. Nakamura. "Energy release rate along a three-dimensional crack front in a thermally stressed body." *International Journal of Fracture* 30, 79-102, (1986).
- [23] K. Sadananda and P. Shahinian, "Fracture mechanics approach to high temperature fatigue crack growth in udimet 700", *Engineering Fracture Mechanics*, 11, 73–86, (1979).
- [24] R.A. Huls, J.F. van Kampen, P. van der Hoogt, J. Kok, Boer de, A. (2008) "Acoustoelastic Interaction in Combustion Chambers: Modeling and Experiments", *Journal of Engineering for Gas Turbines and Power*, 130 (5).
- [25] J. Kok, S. Matarazzo, A. Pozarlik, "The bluff body stabilized premixed flame in an acoustically resonating tube: combustion CFD and measured pressure field", *Proceedings 16th International Congress on Sound and Vibration*, 2009, Krakow, Poland, (2009).
- [26] R.A. Huls, J.F. van Kampen, Jim B.W. Kok and Andre de Boer (2003) "Fluid structure interaction to predict liner vibrations in an industrial combustion system", *ICSV*, 7-10 July 2003 Stockholm Sweden.
- [27] C.E. Feddersen, "Discussion to plane strain crack toughness testing", *ASTM STP*, 410: 77, (1966).
- [28] H. Tada, "A note on the finite width corrections to the stress intensity factor", *Engineering Fracture Mechanics* 3, 345–347, (1971).
- [29] ANSYS®, Academic Research, Release 11.0, Documentation for ANSYS, Elements Reference.
- [30] A.C. Altunlu, P. van der Hoogt, A. de Boer, "Damage evolution by using the near-tip fields of a crack in gas turbine liners", In: *17th International Congress on Sound & Vibration*, ICSV 17, July 18-22, 2010, Cairo, Egypt, (2010).
- [31] R.D. Blevins. *Formulas for natural frequency and mode shape*. Robert E. Krieger publishing company, (1984).
- [32] J.C. Roman Casado, R. Alemela, J. Kok, "Combustion dynamics coupled to structural vibrations", In: *17th International Congress on Sound & Vibration*, ICSV 17, July 18-22, 2010, Cairo, Egypt, (2010).
- [33] K. Bhalla, A. Zehnder and X. Han, "Thermomechanics of slow stable crack growth: closing the loop between experiments and computational modeling", *Engineering Fracture Mechanics*, 70, 2439–2458, (2003).